Localization of adipocyte long-chain fatty acyl-CoA synthetase at the plasma membrane

Christina E. Gargiulo, Sarah M. Stuhlsatz-Krouper, and Jean E. Schaffer[1]

Center for Cardiovascular Research, Department of Internal Medicine and Department of Molecular Biology and Pharmacology, Washington University School of Medicine, St. Louis, MO, 63110-1010

Abstract **Long-chain fatty acyl-CoA synthetase (FACS) catalyzes esterification of long-chain fatty acids (LCFAs) with coenzyme A (CoA), the first step in fatty acid metabolism. FACS has been shown to play a role in LCFA import into bacteria and implicated to function in mammalian cell LCFA import. In the present study, we demonstrate that FACS overexpression in fibroblasts increases LCFA uptake, and overexpression of both FACS and the fatty acid transport protein (FATP) have synergistic effects on LCFA uptake. To explore how FACS contributes to LCFA import, we examined the subcellular location of this enzyme in 3T3-L1 adipocytes which natively express this protein and which efficiently take up LCFAs. We demonstrate for the first time that FACS is an integral membrane protein. Subcellular fractionation of adipocytes by differential density centrifugation reveals immunoreactive and enzymatically active FACS in several membrane fractions, including the plasma membrane. Immunofluorescence studies on adipocyte plasma membrane lawns confirm that FACS resides at the plasma membrane of adipocytes, where it co-distributes with FATP. Taken together, our data support a model in which imported LCFAs are immediately esterified at the plasma membrane upon uptake, and in which FATP and FACS function coordinately to facilitate LCFA movement across the plasma membrane of mammalian cells.**—Gargiulo, C. E., S. M. Stuhlsatz-Krouper, and J. E. Schaffer. **Localization of adipocyte long-chain fatty acyl-CoA synthetase at the plasma membrane.** ***J. Lipid Res.*** **1999.** 40: **881–892.**

Supplementary key words long-chain fatty acid • acyl-CoA synthetase • adipocyte

Long-chain fatty acyl-CoA synthetase (FACS) catalyzes the esterification or activation of long-chain fatty acids (LCFAs, 10–20 carbons chain length, saturated or unsaturated). In this initial step, which is required for all cellular LCFA utilization, a coenzyme A (CoA) moiety is linked in an ATP-dependent reaction to the 1-carbon of an LCFA via a thioester linkage (for recent review, see ref. 1). The acyl-CoA esters are substrates for β-oxidation, phospholipid and triglyceride biosynthesis (2), and protein acylation (3, 4). Acyl-CoA esters have also been proposed to play a role in enzyme activation (5, 6), vesicular trafficking (7, 8), cell signaling (5, 9), modulation of neutrophil function (10), and activation of a ryanodine-like receptor involved in Ca^{2+}-induced Ca^{2+} release in pancreatic acinar cells (11). In addition, acyl-CoA esters have been implicated as ligands for the transcriptional factors HNF-4α (12) and FadR (13).

In *E. coli*, FACS, encoded by the *fadD* gene, is essential for import of exogenous LCFAs (14–17). Another protein required for LCFA import is the *fadL* gene product, which encodes an outer membrane-bound fatty acid transport protein (18). Mutants in *fadD* or in *fadL* are unable to import LCFAs. FadL binds LCFAs with high affinity (K_d 2.3 × 10^7 M for oleate (C18:$1^{\Delta 9}$)) and is thought to transfer them across the outer bacterial membrane via a specific hydrophobic channel that is accessible only upon ligand binding (16, 19–24). FadD is thought to be soluble and loosely associated with the inner bacterial membrane (15, 25). It has been proposed that fadD catalyzes LCFA activation concomitant with transport in a process termed vectorial acylation (14). Two additional proteins, the periplasmic Tsp and an inner membrane bound fatty acid/H^+co-transporter have been postulated to facilitate LCFA transport in *E. coli*, although these proteins are not essential for transport (26–28).

LCFA transport and esterification may also be coupled in mammalian cells to promote efficient LCFA import. Both the murine adipocyte FACS (acyl-CoA synthetase 1, ACS1) and fatty acid transport protein (FATP) were identified in an expression cloning screen, based on the ability of each protein to facilitate LCFA uptake when expressed in COS7 cells (29). FATP is a novel adipocyte 63 kDa plasma membrane protein that increases LCFA uptake by an ATP-dependent mechanism (30). FATP has

Abbreviations: FACS, fatty acyl-CoA synthetase; LCFA, long-chain fatty acids; CoA, coenzyme A; FATP, fatty acid transport protein; DMEM, Dulbecco's modified Eagle's medium; SDS-PAGE, sodium dodecylsulfate-polyacrylamide gel electrophoresis; PBS, phosphate-buffered saline; BSA, bovine serum albumin; PPAR, peroxisome proliferator-activated receptor; PMSF, phenylmethylsulfonyl fluoride; BCA, bicinchoninic acid; LCAD, long-chain acyl-CoA dehydrogenase.

[1] To whom correspondence should be addressed.

been postulated to mediate bi-directional transport of LCFAs across the plasma membrane of adipocytes (31, 32). Immediate, efficient esterification of imported LCFAs by FACS may promote vectorial movement of LCFAs into cells.

This model for mammalian LCFA transport is supported by several recent findings. FATP expression is upregulated in murine adipose and heart tissue during starvation ((32) and D. Bernlohr, personal communication), consistent with a role for FATP not only in uptake of LCFAs into tissues for metabolism, but also in export of LCFAs from adipose tissue stores during lipolysis. Moreover, transcription of FATP and FACS mRNAs is coordinately induced by PPAR (peroxisome proliferator-activated receptor) activators, and this regulation is associated with concomitant increases in LCFA uptake (33). The proposed coordination of transport and initial metabolism of LCFAs in this model is analogous to the proposed coordinate functions of the GLUT4 glucose transporter and hexokinase in glucose transport in mammalian cells.

In the present study, we examine the role of FACS in LCFA uptake in fibroblasts which stably overexpress this enzyme and in 3T3-L1 adipocytes which natively express FACS. In fibroblasts, FACS increases LCFA import and its function is synergistic with the effects of FATP. To explore how FACS functions in LCFA uptake, we characterize the subcellular localization of this enzyme in 3T3-L1 adipocytes. Our findings are consistent with a model in which FACS and FATP function coordinately at the plasma membrane of adipocytes to promote efficient LCFA import.

METHODS

Materials

3T3-L1 cells were obtained from the American Type Culture Collection. These cells were grown and differentiated as previously described (34) and analyzed between days 7 and 13 of differentiation. NIH 3T3 cells were obtained from the American Type Culture Collection and were grown in Dulbecco's modified Eagle's medium (DMEM) supplemented with 10% calf serum, 50 units/ml streptomycin, 50 units/ml penicillin G, 2 mm l-glutamine, and 1 mm sodium pyruvate. [^{14}C]oleic acid was purchased from New England Nuclear. Goat anti-rabbit IgG coupled to a 5 nm gold particle and silver precipitation reagents were purchased from Amersham. Cy-3 donkey anti-rabbit IgG was purchased from Jackson Labs. Horseradish peroxidase-coupled secondary antibodies were purchased from Amersham. Polyclonal rabbit G_β antiserum was purchased from Santa Cruz Biotechnology (SC-378); polyclonal rabbit LCAD antiserum was a gift from A. Strauss (Washington University); polyclonal rabbit γ-adaptin antiserum was a gift from L. Traub (Washington University); polyclonal rabbit PMP70 antiserum was a gift from D. Valle (Johns Hopkins); polyclonal rabbit GLUT4 antiserum was a gift from M. Mueckler (Washington University). BODIPY3823 (4,4-difluoro-5-methyl-4-bora-3α,4α-diaza-3-indacene-3-dodecanoic acid) was obtained from Molecular Probes.

Generation of N-FACS antiserum

A polyclonal rabbit antiserum was raised against the amino-terminus of FACS using a synthetic peptide containing residues 65–77 (N-FACS) of the rat liver FACS sequence. The peptide was coupled to keyhole limpet hemocyanin and immunizations were performed using RIBI IMPL plus TDM plus CWS emulsion, a synthetic adjuvant (Ribi Immunochem Research). The polyclonal rabbit antiserum was prepared as previously described (29). For immunofluorescence studies, affinity-purified antibody was prepared using a column with the N-FACS peptide immobilized on Sulfo-link coupling gel (Pierce) according to the manufacturer's specifications.

Stable cell lines

Murine adipocyte FACS was subcloned into the ΔU3 retroviral expression vector (ΔU3FACS) and transiently transfected into 293GPG packaging cells to produce high titer VSV-G pseudotyped retrovirus as previously described (35). NIH 3T3 cells (10^5) were plated in a 35-mm well and underwent two 7-h infections with 1 ml of the ΔU3FACS retrovirus on consecutive days. Retrovirally transduced populations of NIH 3T3 cells were plated at limiting dilution to allow isolation of independent clonal cell lines. Individual cell lines were screened for FACS expression by Western blot analysis of membrane proteins (pelleted at 356,000 *g*). Similar methods were used to generate cell lines that overexpress FATP or FACS/FATP using a ΔU3 FATP construct and NIH 3T3 cells or FACS-overexpressing cells, respectively.

Western blot analysis

Cellular proteins for Western blot analysis were solubilized in 1% Triton-X 100/ 150 mm NaCl/50 mm Tris-HCl/2 mm EDTA/ 60 mm octylglucoside (TNET-octylglucoside) for antibody characterization or were prepared by subcellular fractionation (see below). Proteins were quantified using the Pierce BCA assay. Equivalent amounts of protein were separated by 7.5% sodium dodecyl-sulfate polyacrylamide gel electrophoresis (SDS-PAGE) and transferred to nitrocellulose membranes (0.2 μm pore). After blocking (5% nonfat dry milk) and primary antibody incubations, membranes were incubated with horseradish peroxidase-coupled donkey anti-rabbit IgG and bands were detected by chemiluminescence.

Fatty acid uptake assays

Fluorescent fatty acid uptake assays were performed as previously described (29). In brief, approximately 1×10^6 cells were trypsinized, washed in serum-free media, and incubated in phosphate-buffered saline (PBS) containing 20 μm bovine serum albumin (BSA) and 0.6 μm BODIPY3823 at 37°C for 1 min. Cells were washed at 4°C with ten volumes of PBS containing 0.1% BSA and 500 μm phloretin and pelleted by centrifugation. Cells were resuspended in complete DMEM media containing 1 μm propidium iodide for flow cytometric analysis on a Becton Dickinson FACScan.

Alkaline extraction of 3T3-L1 proteins

All manipulations were carried out at 4°C. Cells were washed twice in PBS and once in 150 mm NaCl. Cells were scraped in SHB (20 mm Tris-HCl, pH 7.4, 1 mm EDTA/255 mm sucrose), 0.1 m Na_2CO_3, 0.8 m KAc, or 1% Triton X-100, each containing 1 μg/ml leupeptin, 1 mm phenylmethylsulfonyl fluoride (PMSF), and 1 μg/ml pepstatin A. Cells were homogenized with 20 strokes in a Teflon-glass homogenizer. Nuclei and unbroken cells were removed by centrifugation at 1000 *g* for 10 min. Membranes were pelleted by centrifugation at 356,000 *g* for 30 min and resuspended in their respective homogenization buffers. Proteins from soluble and membrane fractions were precipitated with 1 volume chloroform and 0.25 volumes methanol. The pellets were washed with methanol, resuspended in 1% SDS, and quantified using the bicinchoninic acid (BCA) assay (Pierce). Twenty-five

μg of protein from each sample was separated by SDS-PAGE and analyzed by Western blot.

Subcellular fractionation

Adipocytes were fractionated according to the protocol of Simpson et al. (36) with slight modifications. All manipulations were performed at 4°C. Cells were washed and scraped in SHB containing 1 μg/ml leupeptin/1 mm PMSF/and 1 μg/ml pepstatin A. Cells were homogenized with 20 strokes in a Teflon-glass homogenizer. Nuclei and unbroken cells were pelleted by centrifugation at 1000 *g* for 10 min. The post-nuclear supernatant was centrifuged at 16,000 *g* for 20 min. The pellet was resuspended in SHB, layered onto a sucrose cushion (1.12 m sucrose/1 mm EDTA/ and 20 mm Tris-HCl, pH 7.4) and centrifuged at 101,000 *g* for 25 min to yield a mitochondrial/peroxisomal pellet with plasma membranes at the interface. The 16,000 *g* supernatant was centrifuged at 48,000 *g* for 20 min to yield a high density microsome pellet and a supernatant that was centrifuged at 356,000 *g* for 45 min to yield a low density microsome pellet and a supernatant containing the cytosol. Membranes were resuspended in SHB for Western blot analysis or in buffer containing 20 mm potassium phosphate, pH 7.4/ 2 mm Triton X-100/ 5 mm β-mercaptoethanol/1 μg/ml leupeptin/ 1 mm PMSF/ and 1 μg/ml pepstatin A for FACS activity assays. Proteins were quantified by BCA assay (Pierce).

FACS activity assay

3T3-L1 cells were fractionated as described above and membrane microsomes were analyzed as described previously (37). In brief, 50 μg protein from each fraction was incubated for 2 min with [^{14}C]oleic acid in the presence of ATP, Mg^{2+}, and CoA. Reactions were stopped and the [^{14}C]oleoyl-CoA was separated from unreacted [^{14}C]oleic acid by heptane extraction and quantified by scintillation counting. Separation of the free fatty acid from the CoA ester is based on the relative solubility of acyl-CoAs in the aqueous phase and the relative solubility of unreacted LCFAs in the organic phase. These assays were performed in triplicate in three independent experiments. Esterification was linear with increasing amounts of 3T3-L1 adipocyte microsomes up to 125 μg protein per reaction (J. E. Schaffer, unpublished data).

Immunofluorescence of 3T3-L1 adipocytes

3T3-L1 adipocytes were differentiated on glass coverslips. Plasma membrane lawns were prepared as previously described (38–40). In brief, cells were washed with PBS, with Ca^{2+}-free Ringers (155 mm NaCl/ 3 mm KCl/ 5 mm $MgCl_2$/ 3 mm NaH_2PO_4/ 5 mm HEPES/ 10 mm glucose/ 3 mm EGTA), and with Ca^{2+}-free Ringers supplemented with 0.1 mg/ml poly-l-lysine. Cells were swelled in a hypotonic buffer (70 mm KCl/ 30 mm HEPES/ 5 mm $MgCl_2$/ 3 mm EGTA) and sonicated in hypotonic buffer supplemented with 1 mm DTT, 0.1 mm PMSF, and 4% paraformaldehyde. Cells were sonicated for 2 sec with a Kontes micro-ultrasonic (power setting 3.5) or a Microson XL sonicator using a probe with a diameter of 0.3 cm centered 0.3 cm above the cells. Lawns were fixed for 30 min in the hypotonic buffer supplemented with 4% paraformaldehyde, washed in PBS, and blocked by incubation with 200 μg/ml goat IgG. Primary antibody incubations were performed at 25°C for 1 h with affinity-purified rabbit polyclonal primary antibodies directed against FACS (N-FACS 1:25) or FATP (C-FATP 1:50 (29)) or with a rabbit polyclonal antiserum directed against GLUT4 (10 μg/ml). As a control, 100 μg/ml of immunizing peptide was pre-incubated with the antiserum for some incubations. After washing in PBS, secondary antibody incubations were performed for 1 h at 25°C with Cy-3-conjugated donkey anti-rabbit IgG (FATP and GLUT4) or goat anti-rabbit IgG coupled to a 5-nm gold particle (FACS). For detection of the gold particles a silver enhancement was performed according to the manufacturer's specifications at 28°C for 15 min (Amersham). The silver precipitation reactions resulted in fixation of the primary antibody, masking it in subsequent secondary antibody incubations in double staining experiments. After staining, slides were extensively washed in PBS, examined by both immunofluorescence and polarized light microscopy, and photographed.

RESULTS

Generation of anti-FACS antiserum

To facilitate studies of FACS, we generated a rabbit polylconal anti-peptide antiserum directed against FACS amino acid residues 65–77 (N-FACS), sequence not conserved in ACS2, 3, or 4. The antiserum was first tested for its ability to recognize the 78 kDa FACS by Western blot. We used proteins prepared from NIH 3T3 cells (which have undetectable FACS activity and undetectable FACS mRNA by Northern blot analysis, J. E. Schaffer and S. M. Stuhlsatz-Krouper, unpublished results), from an NIH 3T3 cell line that overexpresses FACS, and from 3T3-L1 adipocytes that natively express this protein (7, 41). Western blot analysis (**Fig. 1**) demonstrates that a single band at the predicted molecular weight of 78 kDa is observed in FACS-overexpressing cells (lanes 2) and in 3T3-L1 adipocytes (lanes 3), but not in parental NIH 3T3 cells (lanes 1). The FACS signal is competed for by pre-incubation of the antiserum with its immunizing peptide, but not by pre-incubation with an irrelevant peptide (FACS residues 676-689). These results demonstrate that the N-FACS specifically recognizes the adipocyte FACS protein.

FACS contributes to LCFA uptake

To characterize the role of FACS in cellular LCFA uptake, we generated stable cell lines that overexpress FACS, FATP, and both FACS/FATP (co-expressing) in an NIH 3T3 cell background. Clonal cell lines were screened for expression of these proteins by Western blot (**Fig. 2A**). A strong signal for FACS is detected only in the FACS and co-expressing cell lines. FATP is expressed at low levels in NIH 3T3 cells and in FACS-overexpressing cells, but a

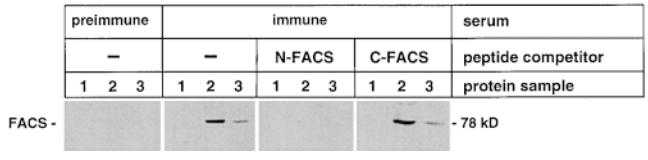

Fig. 1. Characterization of anti-FACS antiserum. Twenty μg of protein from NIH 3T3 cells, FACS-overexpressing cells, and 3T3-L1 adipocytes were separated by SDS-PAGE (7.5%) in lanes 1, 2, and 3, respectively. Proteins were transferred to nitrocellulose membranes and incubated with pre-immune or immune sera (1:1000 dilution). Western blot analysis was performed using a rabbit polyclonal anti-peptide antiserum raised against the amino terminus of FACS. Bands were detected using a horseradish peroxidase-coupled anti-rabbit IgG and chemiluminescence. As a control, the immunizing amino-terminus peptide (residues 65–77) and a carboxyl-terminus peptide (residues 676–689) were included in the indicated incubations at a concentration of 50 μg/ml.

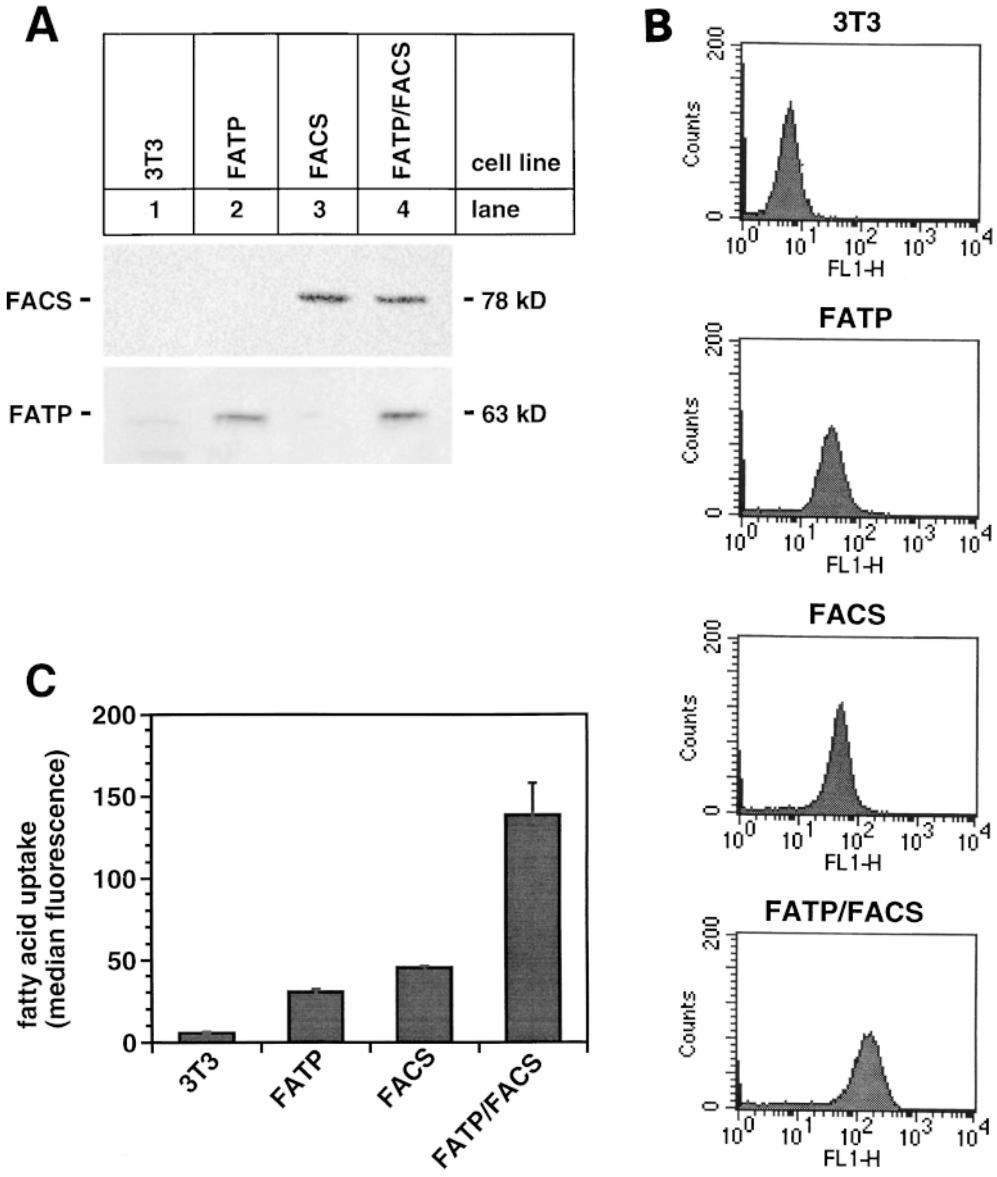

Fig. 2. Effects of FACS and FATP on LCFA uptake. A: Stable FATP-, FACS-, and FATP/FACS-overexpressing cell lines were generated as described in Methods. From each cell line 20 μg of membrane protein was separated by SDS-PAGE (7.5%) and incubated with either the N-FACS (1:1000) or the C-FATP antiserum (1:1000). Bands were detected using a horseradish peroxidase-coupled IgG and chemiluminescence. B: Cell lines were evaluated for 1 min uptake of a fluorescent fatty acid analog as described in Methods. For each cell line tested, histograms display fluorescence on a log scale on the x-axis (FL-1-H) and cell number on the y-axis (counts) for 10^5 cells. C: Bar graph displays the median fluorescence of each cell line shown in B. Assay was performed in triplicate and the results are representative of 3 independent experiments.

stronger FATP signal is observed in the FATP- and co-expressing cell lines. The level of expression of each protein in its single protein-overexpressing cell line is comparable to the level in the co-expressing cell line. Moreover, overexpression of either protein alone did not alter the basal level of expression of the other protein in the NIH 3T3 cell background.

We tested these cell lines for fatty acid uptake using the fluorescent fatty acid analog, BODIPY3823. In adipocytes and in cell lines overexpressing FATP, uptake of this fatty acid analog is comparable to uptake of radiolabeled oleic acid (29, 42), and oleic acid effectively competes with BODIPY3823 for uptake in our cell lines (J. E. Schaffer and S. M. Stuhlsatz-Krouper, unpublished results). Cells were incubated with BODIPY3823 for 1 min, washed to remove surface-bound fatty acid, and analyzed by flow cytometry (Fig. 2B and C). The parental NIH 3T3 cells have low background level of LCFA transport as previously demonstrated (29). Overexpression of FATP confers a 6-fold increase in fatty acid uptake compared to the parental NIH 3T3 cells. Overexpression of FACS yields an 8-fold increase in uptake. Overexpression of both proteins confers a 25-fold increase in uptake. These findings were confirmed using several independent panels of clonal overex-

pressing cell lines. The observation that co-expression leads to a synergistic increase in LCFA uptake is consistent with a functional interaction between FACS and FATP.

FACS is an integral membrane protein

To understand how FACS might contribute to LCFA import, we characterized the subcellular localization of FACS in 3T3-L1 adipocytes. Hydropathy analysis of the amino acid sequence of FACS following the Kyte Doolittle algorithm (43) shows that FACS has significant hydrophobic regions of sequence (**Fig. 3A**). For this analysis we used a window of 17 amino acids, the minimum number of residues required for an α-helix to span a phospholipid bilayer (43). Because there are several regions of significantly hydrophobic sequence (displayed as positive values in the plot), we hypothesized that FACS is an integral membrane protein. FACS, however, is an enzyme that interacts with amphipathic substrates. Hydrophobic regions in this sequence may instead correspond to regions of FACS that bind or interact with LCFAs.

To determine experimentally whether FACS is an integral membrane protein, 3T3-L1 adipocytes were homogenized and extracted in high salt or detergent-containing buffers. Soluble (S) and membrane (P) fractions were separated by centrifugation and analyzed by Western blot using the N-FACS antiserum (Fig. 3B). FACS remains associated with the alkaline- and high salt-inextractable membrane fractions of adipocytes. FACS is solubilized in 1% Triton-X 100. These findings suggest that FACS is an integral membrane protein.

FACS is present at the adipocyte plasma membrane

To determine which membranes of 3T3-L1 adipocytes contain FACS, mature adipocytes were fractionated by differential density centrifugation to yield membrane fractions enriched for nuclei (NUC), mitochondria (MIT), plasma membrane (PM), high density microsomes (HDM, containing endoplasmic reticulum (ER), trans-Golgi network, and endosomes), low density microsomes (LDM, containing Golgi apparatus, secretory vesicles and endosomes), and cytosol (36). Western blot analysis of these fractions using the N-FACS anti-peptide antiserum shows FACS predominantly in the PM and HDM fractions, and smaller amounts of FACS in the MIT and NUC fractions (**Fig. 4A**). To assess the purity of our fractions, we analyzed the distribution of proteins known to reside within specific intracellular compartments. γ-Adaptin, a Golgi protein involved in vesicular trafficking, is enriched in the HDM and LDM fractions and is depleted from the PM. The G protein β subunit (G_β), known to reside in the plasma membrane, is enriched in the PM fraction. Its appearance in the HDM fraction may represent newly synthesized G_β molecules which have not yet reached the PM. The mitochondrial enzyme long chain acyl-CoA dehydrogenase (LCAD) is enriched in the MIT fraction and relatively depleted from the PM. The low LCAD signal in the NUC fraction likely represents contamination of the NUC fraction by mitochondria or unbroken cells. The 70 kDa peroxisomal membrane protein is observed in the MIT, NUC and LDM fractions, but is depleted from the PM. These controls demonstrate that our PM fraction is enriched for plasma membrane proteins and is relatively depleted of nuclear, mitochondrial, Golgi, and peroxisomal proteins.

We also analyzed 50 μg protein from each membrane fraction for FACS enzymatic activity by the isotopic method of Tanaka and coworkers (37). FACS activity parallels the subcellular distribution observed by Western blot analysis, with the highest activities in the PM (36% of total) and HDM (27% of total) fractions and lower level activity in the NUC and MIT fractions (Fig. 4B). Taken together, our Western blot and enzymatic analyses are consistent with the hypothesis that the FACS activity present in diverse cellular membranes represents multiple subcel-

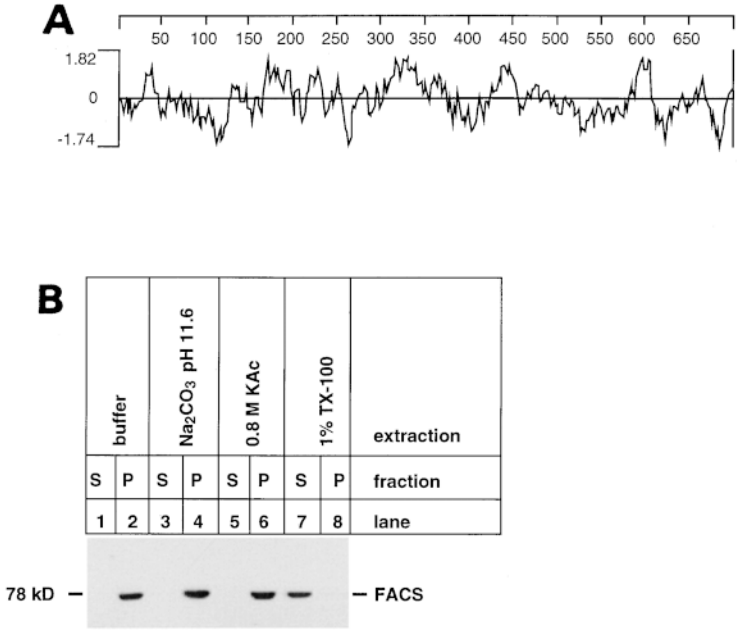

Fig. 3. FACS is an integral membrane protein. A: Hydropathy plot of the amino acid sequence for FACS followed the method of Kyte and Doolittle (43), using a window of 17 amino acid residues. Regions of hydrophobic sequence are displayed as positive values in this plot, generated using DNASTAR software. B: Western blot analysis shows alkaline and high salt extractions of 3T3-L1 adipocyte proteins. Cells were disrupted by homogenization in a sucrose-Tris-EDTA buffer (lanes 1 and 2), 0.1 M Na_2CO_3 (lanes 3 and 4), 0.8 M KAc (lanes 5 and 6), or 1% Triton X-100 (lanes 7 and 8). Soluble (S) and membrane (P) fractions were separated by centrifugation, precipitated, and quantified. Twenty-five μg of protein from each fraction was separated by SDS-PAGE (7.5%) and transferred to nitrocellulose. FACS was detected using the N-FACS antiserum, a horseradish peroxidase-coupled anti-rabbit IgG, and chemiluminescence.

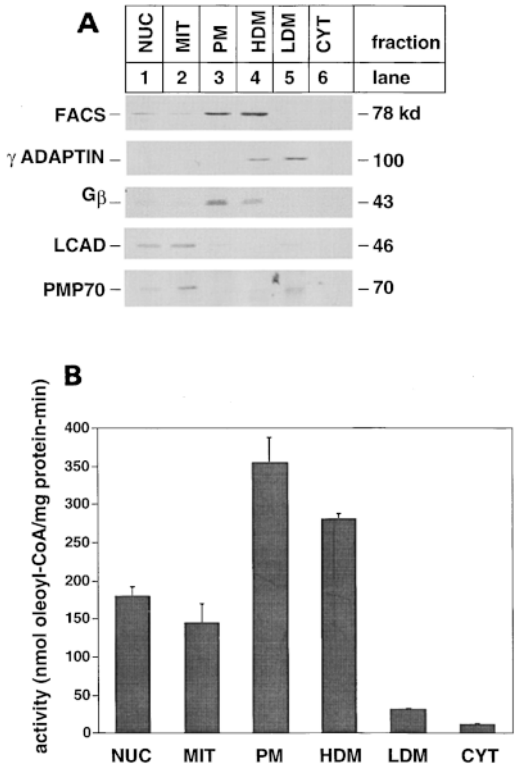

Fig. 4. Localization of FACS in adipocytes by subcellular fractionation. 3T3-L1 adipocytes were disrupted by homogenization and fractionated by differential density centrifugation. A: For Western blot analysis, 40 μg protein from each fraction was separated by SDS-PAGE (7.5%) and transferred to nitrocellulose. For detection of FACS we used the N-FACS antiserum, a horseradish peroxidase-coupled anti-rabbit IgG, and chemiluminescence. Rabbit polyclonal antisera against γ-adaptin, the G protein β subunit (G_β), long-chain acyl-CoA dehydrogenase (LCAD), and the 70 kD peroxisomal membrane protein (PMP70) were used to assess the enrichment of the various fractions. Fractions are designated nucleus (NUC), mitochondrial (MIT), plasma membrane (PM), high density microsomes (HDM), low density microsomes (LDM), and cytosol (CYT). B: Fifty μg protein from each cell fraction was assayed for FACS activity. Reactions were performed in triplicate, and the data shown are representative of several independent experiments.

lular locations for this enzyme, including the PM. The enrichment of FACS activity in the PM and HDM fractions is less than the enrichment of immunoreactive FACS in the PM and HDM fractions by Western blot analysis. This difference may be the result of greater sensitivity of the enzymatic assay, differing kinetic properties of FACS molecules in different subcellular locations, or the presence of other proteins with FACS activity in the NUC and MIT fractions.

To confirm that FACS resides at the plasma membrane of adipocytes, we performed immunofluorescence microscopy. In preliminary experiments, the N-FACS anti-peptide antiserum did not stain live 3T3-L1 adipocytes, but demonstrated specific staining in multiple membrane compartments of fixed, permeabilized 3T3-L1 adipocytes, consistent with our detection of FACS in several subcellular fractions (data not shown). We then used the plasma membrane lawn technique to specifically examine whether FACS is present in adipocyte plasma membranes. In this method, cells are grown on glass coverslips, swollen in a hypotonic buffer, and sonicated to break open cells, allowing intracellular contents to wash away and leaving the plasma membrane attached to the substratum. This technique has been elegantly used to examine a number of plasma membrane proteins, including the GLUT4 glucose transporter whose translocation from LDMs to PM can be shown in lawns prepared from unstimulated (with minimal staining for GLUT4) and insulin-stimulated (with intense staining for GLUT4) adipocytes (39, 44).

We isolated plasma membrane lawns from 3T3-L1 adipocytes incubated in the presence or absence of 1 μm insulin. Using the affinity-purified N-FACS antibody, we observed a highly abundant punctate staining pattern in the PM lawns prepared from insulin-treated (**Fig. 5A**) and untreated 3T3-L1 adipocytes (5C). This staining is specific, as it is not seen with peptide competitor (5G) or with secondary antibody alone (5E). Localization of FACS in the plasma membrane lawn was not affected by pre-incubation of the cells with insulin (compare 5A and 5C). As a control for the adequacy of our plasma membrane lawn preparation, we also stained for the GLUT4 glucose transporter. Insulin-stimulated translocation of GLUT4 was readily observed (compare 5B and 5D). The absence of GLUT4 staining under basal conditions (5D) shows that our plasma membrane lawns do not contain intracellular GLUT4-containing vesicles. These immunocytochemistry studies are in agreement with our subcellular fractionation data and strongly suggest that the enzyme FACS is natively associated with the plasma membrane of adipocytes.

FACS co-distributes with FATP

Our finding of FACS at the adipocyte plasma membrane suggested that FACS and FATP, previously shown to be an integral plasma membrane protein, may co-distribute to areas of the plasma membrane specialized for LCFA uptake. To test this hypothesis, we stained adipocyte plasma membrane lawns for both FACS and FATP (**Fig. 6**). The same field of view was stained for FACS (A), FATP (C) and both proteins (E). The staining for each protein is specific, with no signal observed using excess immunizing peptide as competitor (B and D) or secondary antibody alone (F and G). The patterns of FACS and FATP staining almost completely overlap to give a white color on double exposure. Neither FACS nor FATP co-distribute with caveolin and neither protein is Triton-insoluble (data not shown). The co-distribution of FACS and FATP staining is consistent with a model in which FATP and FACS function coordinately in LCFA uptake.

DISCUSSION

To assess the potential role of FACS in mammalian cell LCFA transport, we examined the function of this enzyme in stably overexpressing NIH 3T3 cells. FACS facilitates LCFA import in these cells, and functions synergistically with FATP. Toward understanding how the intracellular FACS contributes to LCFA import, we determined the sub-

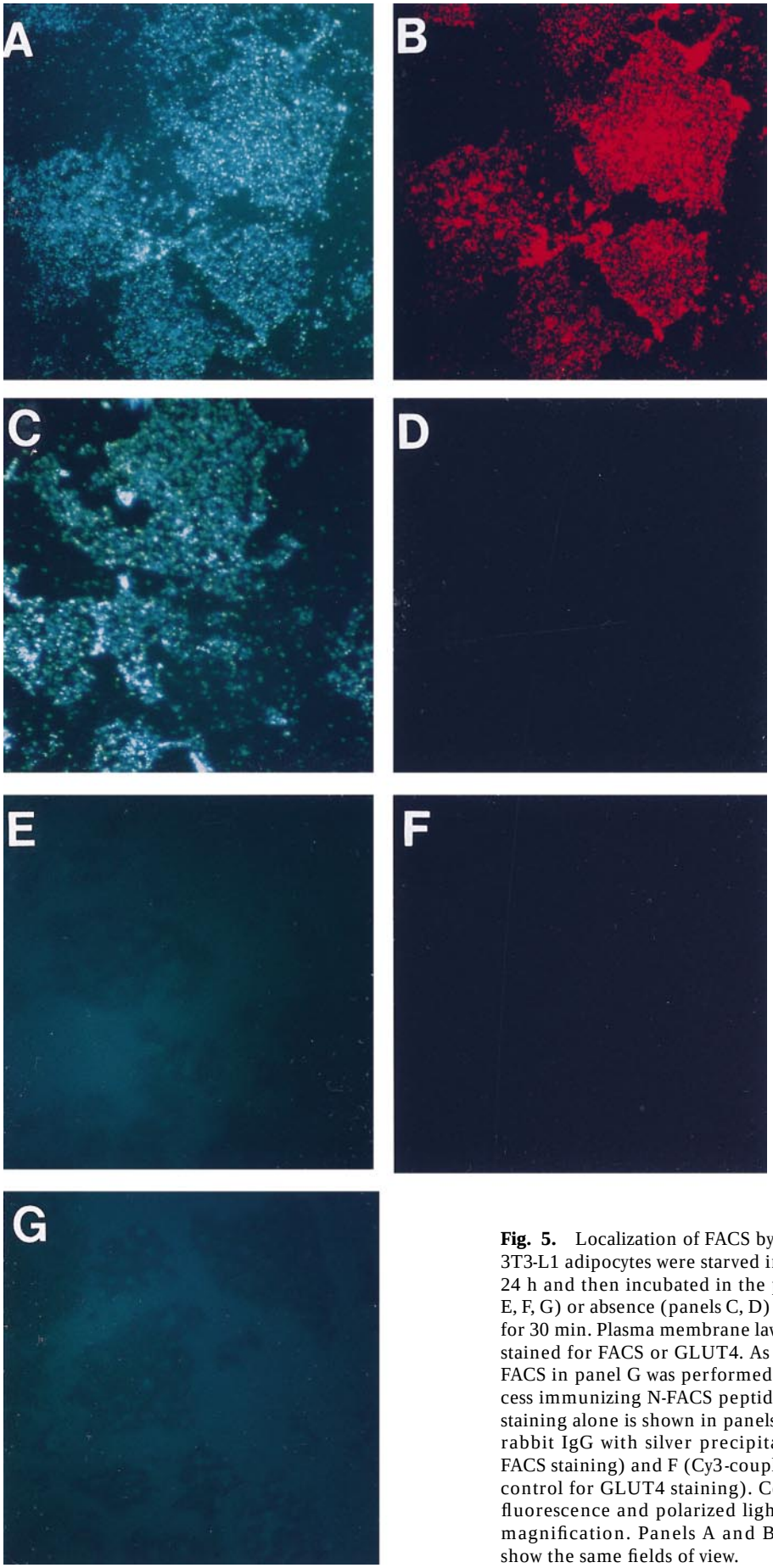

Fig. 5. Localization of FACS by immunofluorescence. 3T3-L1 adipocytes were starved in serum-free media for 24 h and then incubated in the presence (panels A, B, E, F, G) or absence (panels C, D) of 1 μm insulin at 37°C for 30 min. Plasma membrane lawns were prepared and stained for FACS or GLUT4. As a control, staining for FACS in panel G was performed in the presence of excess immunizing N-FACS peptide. Secondary antibody staining alone is shown in panels E (gold-coupled anti-rabbit IgG with silver precipitation as a control for FACS staining) and F (Cy3-coupled anti-rabbit IgG as a control for GLUT4 staining). Cells were examined by fluorescence and polarized light microscopy at 630× magnification. Panels A and B and panels C and D show the same fields of view.

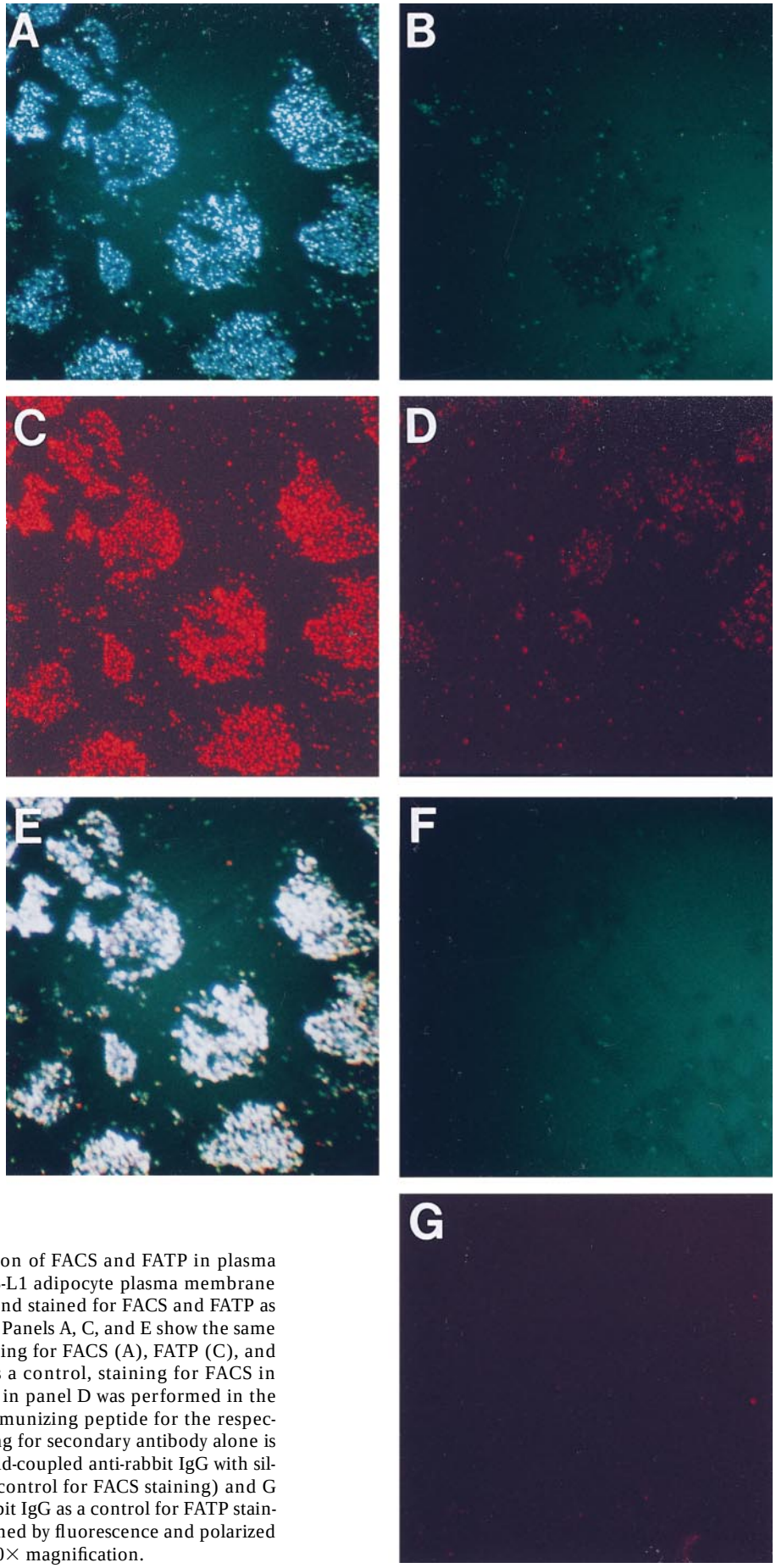

Fig. 6. Co-distribution of FACS and FATP in plasma membrane lawns. 3T3-L1 adipocyte plasma membrane lawns were prepared and stained for FACS and FATP as described in Methods. Panels A, C, and E show the same field of view with staining for FACS (A), FATP (C), and both proteins (E). As a control, staining for FACS in panel B and for FATP in panel D was performed in the presence of excess immunizing peptide for the respective antibodies. Staining for secondary antibody alone is shown in panels F (gold-coupled anti-rabbit IgG with silver precipitation as a control for FACS staining) and G (Cy3-coupled anti-rabbit IgG as a control for FATP staining). Cells were examined by fluorescence and polarized light microscopy at 630× magnification.

cellular localization of this enzyme in 3T3-L1 adipocytes, which natively express FACS at high levels. We demonstrate for the first time that FACS is an integral membrane protein. Moreover, we show that FACS is associated with the plasma membrane of adipocytes, where it co-distributes with FATP. Taken together, our findings are consistent with a model in which LCFA uptake is functionally coupled to esterification of the imported LCFAs directly at the plasma membrane of adipocytes.

While enzymatic FACS activity has been shown by others to be associated with cellular membranes (45–48), our epitope-specific anti-FACS antibody has facilitated a more detailed molecular characterization of the FACS-membrane association. For generation of the anti-FACS antiserum, we chose a region of the ACS1 amino acid sequence which is not conserved in ACS2, 3, or 4. This permitted examination specifically of the only FACS isoform implicated in LCFA transport. Unlike the prokaryotic fadD which is soluble and loosely associated with membranes (15, 25), adipocyte FACS is an integral membrane protein. Integral association of FACS with membranes may promote interactions of this enzyme with amphipathic LCFA substrates that tend to associate with membranes. Topology mapping and mutational analysis of FACS currently underway in our laboratory will help elucidate the structure–function correlates for this enzyme.

Previously published studies have shown FACS activity associated with a variety of eukaryotic cellular membranes, but these studies have failed to clearly demonstrate FACS at the plasma membrane (45, 46, 48–59). In these studies membranes were fractionated by differential density centrifugation and assayed for enzymatic activity. Adequate controls to assess purity of the membrane fractions were not shown, and subsequent studies have suggested that these membrane fractions were contaminated by peroxisomes, microsomes, and/or mitochondria (1, 60). Because localization was not examined by techniques other than enzymatic assay for esterification in the fractionated membranes, it was not possible to exclude the existence of different enzymes with related activities in the various cellular membranes. In these studies, the level of FACS activity in plasma membranes was a small fraction of total cellular activity (57–59), consistent with contamination from other fractions where FACS activity was significantly more abundant. For these reasons, localization of this enzyme at the plasma membrane has remained controversial.

Based on our findings that FACS contributes significantly to LCFA import into mammalian cells, we hypothesized that this enzyme may be present at the plasma membrane. We used two independent techniques to demonstrate unequivocally that FACS is localized to the plasma membrane. Our subcellular fractionation and immunofluorescence experiments included controls to show that there is minimal contamination of our plasma membrane fractions with peroxisomes (PMP70), mitochondria (LCAD), or microsomes (γ-adaptin) and minimal contamination of our plasma membrane lawns with GLUT4-containing vesicles. We have used a combination of immunochemical (Western blot analysis and immunocytochemistry) and biochemical (enzyme activity assay) methods for detection of FACS in our subcellular fractions. The level of FACS activity and immunologically detectable FACS protein at the adipocyte plasma membrane is comparable to the highest levels detected in the adipocyte HDMs (endoplasmic reticulum), and several orders of magnitude greater than previously reported in erythrocyte and hepatocyte plasma membranes (57–59). Differences between the subcellular localization of FACS in the present study and previously published works may reflect true differences in localization in various cell types, differences in subcellular fractionation techniques, or differences in the efficiency of detection methods.

Co-distribution of FATP and FACS at the adipocyte plasma membrane and the synergistic effects of the two proteins on LCFA uptake in NIH 3T3 cells suggest that these proteins function coordinately to facilitate efficient LCFA import in adipocytes. The functions of FATP and FACS are not likely to be redundant, as the effects of these proteins are not simply additive, and as FACS but not FATP has LCFA esterifying activity (J. E. Schaffer and S. M. Stuhlsatz-Krouper, unpublished observations). Coordination of transport and esterification of LCFAs may not only provide a mechanism for efficient LCFA import, but also for regulation of LCFA import. In *E. coli*, regulation of fatty acid uptake may occur in part by recruitment of FACS to the plasma membrane (61).

The ability of cells to esterify imported LCFAs directly at the plasma membrane has implications for the directionality of LCFA movement across the plasma membrane and for the mechanism of intracellular LCFA trafficking. In our model for LCFA uptake (**Fig. 7A**), bi-directional flux of LCFAs across the plasma membrane is facilitated by FATP (31, 32), and imported LCFAs can be bound to cytosolic fatty acid binding proteins (FABPs). High extracellular LCFA concentrations or overexpression of FATP increases the import of LCFAs. When expressed, a proportion of FACS is trafficked (actively or passively) to the plasma membrane where it esterifies incoming LCFAs (Fig. 7B). Efficient esterification maintains a low intracellular LCFA concentration and contributes to uptake through the establishment of an outside-to-inside LCFA gradient (62). Moreover, esterified LCFAs are trapped within the cell because they are not a substrate for FATP (J. E. Schaffer and S. M. Stuhlsatz-Krouper, unpublished observations). These esterified LCFAs bind to acyl-CoA binding proteins (ACBPs) with high affinity (63). Thus, imported LCFAs can be rapidly incorporated into the cellular acyl-CoA pools, and ACBPs may play a more significant role in the intracellular targeting of these molecules than FABPs. Experiments to test these predictions are currently underway in our laboratory.

Overexpression of FATP and FACS together is likely synergistic because of the combined effects of increased transport and increased capacity to esterify the substrate at the plasma membrane. An FATP–FACS complex might facilitate direct transfer of LCFAs from FATP to FACS; however, co-immunoprecipitation and cross-linking studies in our laboratory have not, to date, revealed a physical

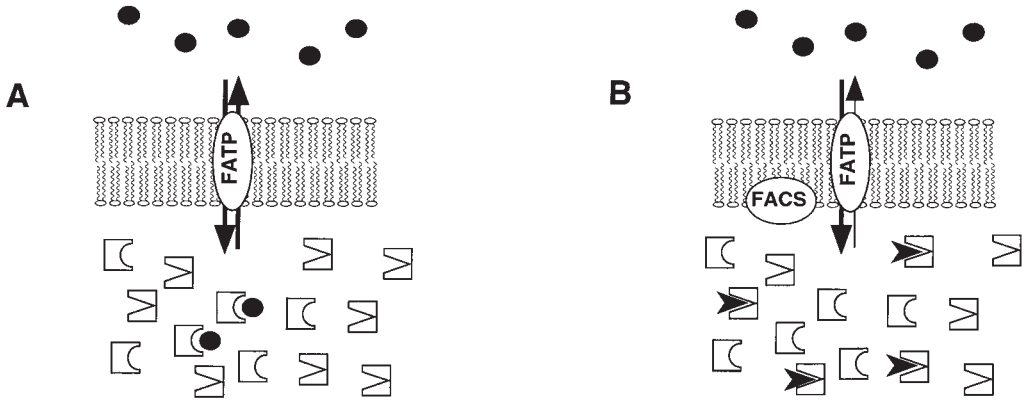

Fig. 7. Model for coordinate FACS and FATP function in LCFA transport. A: In cells without plasma membrane-associated FACS, FATP facilitates bi-directional movement of LCFAs (●) across the plasma membrane. In the cytosol, LCFAs bind to fatty acid binding proteins (FABPs, square with curved indentation). B: In cells with FACS expression at the plasma membrane, imported LCFAs are immediately esterified (arrow heads) at the plasma membrane. LCFA esters bind to acyl-CoA binding proteins (ACBPs, square with triangular indentation).

association between these proteins. Alternatively, FATP and FACS may reside together in specialized, non-caveolar regions of the plasma membrane across which LCFA import occurs without a direct protein–protein interaction. FATP may deliver the LCFA substrate to the inner leaflet of the plasma membrane, in which the LCFA is free to diffuse and come in contact with nearby FACS. By either mechanism, close physical proximity of FATP and FACS could contribute to functional coupling of these proteins and synergistic effects on LCFA import.

Although our studies suggest that FACS plays an important role in adipocyte LCFA import, and although the studies of others have shown that FACS is essential for bacterial LCFA uptake, these effects may be cell-type specific. Studies by Knoll, Johnson, and Gordon (64) suggest that in *Saccharomyces cerevisiae* (*S. cerevisiae*), import and activation of myristate and palmitate are not coupled. Four distinct FACS or fatty acid activation (FAA) genes have been identified in *S. cerevisiae* (64–67). FAA1 and FAA4 preferentially activate the subset of exogenous LCFAs which are imported into yeast cells. Isogenic FAA1FAA4 and *faa1Δfaa4Δ* strains show no differences in rates of transport of these substrates, and complementation of *faa1Δfaa4Δ* with FAA1, FAA4, or the mammalian ACS1 does not increase transport of either fatty acid.

In addition to a potential role in cellular LCFA import, the plasma membrane localization of FACS may facilitate vesicular trafficking in mammalian cells, by providing appropriate acyl chain donors for protein acylation which is critical for membrane budding or fusion. Pfanner and coworkers (8) have shown that a functional FACS and its fatty acyl-CoA products are required for budding of transport vesicles from the Golgi cisternae. More recent experiments from Sleeman and colleagues (7) demonstrate FACS activity in GLUT4-containing vesicles of adipocytes. These vesicles, which comprise approximately 5% of adipocyte LDMs, fuse with the plasma membrane upon insulin stimulation, thereby translocating GLUT4 (and presumably some FACS) to the cell surface to increase glucose uptake. In our experiments, however, we have not observed insulin-mediated changes in adipocyte FACS localization by subcellular fractionation (data not shown) or by immunofluorescence (the present study).

It remains unclear how FACS is localized to several distinct organelles. The present study and those of several groups (52, 68) find no molecular, catalytic, or immunologic differences among FACS associated with different cellular membranes. Alternative translation initiation has been proposed as a mechanism for generating different FACS isoforms with heterogeneous amino termini (69), even though specific translation start sites have not been associated with particular subcellular localizations. The complex localization of FACS in several cellular membranes may allow this enzyme to esterify selective LCFA pools depending on location or to generate acyl-CoA esters which are efficiently targeted to different cellular fates as a function of location. Studies to elucidate the mechanisms of subcellular targeting of FACS and the mechanisms of interaction between this enzyme and substrates will contribute greatly to our understanding of fatty acid homeostasis.

We thank D. Ory, J. Gordon, D. Kelly, J. Saffitz, A. Strauss, and R. Wells for helpful discussions and critical review of this manuscript. We are grateful to J. Heuser and M. Mueckler for assistance with plasma membrane lawn studies. C.E.G. is supported by the Lucille P. Markey Foundation. Support for this work was also provided by a grant from the National Institute of Diabetes and Digestive and Kidney Diseases (DK54268).

Manuscript received 14 December 1998.

REFERENCES

1. Watkins, P. A. 1997. Fatty acid activation. *Prog. Lipid Res.* **36:** 55–83.
2. Waku, K. 1992. Origins and fates of fatty acyl-CoA esters. *Biochim. Biophys. Acta.* **1124:** 101–111.
3. Berger, M., and M. F. G. Schmidt. 1984. Identification of acyl donors and acceptor proteins for fatty acid acylation in BHK cells infected with Semliki Forest virus. *EMBO.* **3:** 713–719.

4. Bhatnagar, R. S., O. F. Schall, E. Jackson-Machelski, J. A. Sikorski, B. Devaadas, G. W. Gokel, and J. I. Gordon. 1997. Titration calorimetric analysis of acyl-CoA recognition by myristoylCoA: protein N-myristoyltransferase. *Biochemistry.* **36:** 6700–6708.
5. Faergeman, N. J., and J. Knudsen. 1997. Role of long-chain fatty acyl-CoA esters in the regulation of metabolism and in cell signaling. *Biochem. J.* **323:** 1–12.
6. Liu, Y. Q., K. Tornhiem, and J. L. Leahy. 1998. Fatty acid-induced β-cell hypersensitivity to glucose. *J. Clin. Invest.* **101:** 1870–1875.
7. Sleeman, M. W., N. P. Donegan, R. Heller-Harrison, W. S. Lane, and M. P. Czech. 1998. Association of acyl-CoA synthetase-1 with GLUT4-containing vesicles. *J. Biol. Chem.* **273:** 3132–3135.
8. Pfanner, N., L. Orci, B. S. Glick, M. Amherdt, S. R. Arden, V. Malhotra, and J. E. Rothman. 1989. Fatty acyl-coenzyme A is required for budding of transport vesicles from Golgi cisternae. *Cell.* **59:** 95–102.
9. Bronfman, M., M. N. Morales, and A. Orellana. 1988. Diacylglycerol activation of Protein Kinase C is modulated by long-chain acyl-CoA. *Biochem. Biophys. Res. Commun.* **152:** 987–992.
10. Korchak, H. M., L. H. Kane, M. W. Rossi, and B. E. Corkey. 1994. Long chain acyl-coenzyme A and signaling in neutrophils. *J. Biol. Chem.* **269:** 30281–30287.
11. Fitzsimmons, T. J., J. A. McRoberts, K. H. Tachiki, and S. J. Pandol. 1997. Acyl-coenzyme A causes Ca^{2+} release in pancreatic acinar cells. *J. Biol. Chem.* **272:** 31345–31350.
12. Hertz, R., J. Magenheim, I. Berman, and J. Bar-Tana. 1998. Fatty acyl-CoA thioesters are ligands of hepatic nuclear factor 4α. *Nature.* **392:** 512–516.
13. Raman, N., P. N. Black, and C. DiRusso. 1997. Characterization of the fatty-acid responsive transcription factor FadR. *J. Biol. Chem.* **272:** 30645–30650.
14. Klein, K., R. Steinberg, B. Fiethen, and P. Overath. 1971. Fatty acid degradation in *Escherichia coli*. An inducible system for the uptake of fatty acids and further characterization of old mutants. *Eur. J. Biochem.* **19:** 442–450.
15. Kameda, K., and W. D. Nunn. 1981. Purification and characterization of acyl coenzyme A synthetase from *Escherichia coli*. *J. Biol. Chem.* **256:** 5702–5707.
16. Black, P. N., C. C. DiRusso, A. K. Metzger, and T. L. Heimert. 1992. Cloning, sequencing, and expression of the *fadD* gene of *Escherichia coli* encoding the acyl coenzyme A synthetase. *J. Biol. Chem.* **267:** 25513–25520.
17. Black, P. N., Q. Zhang, J. D. Weimar, and C. C. DiRusso. 1997. Mutational analysis of a fatty acyl–coenzyme A synthetase signature motif identifies seven amino acid residues that modulate fatty acid substrate specificity. *J. Biol. Chem.* **272:** 4896–4903.
18. Maloy, S. R., C. L. Ginsburgh, R. W. Simons, and W. D. Nunn. 1981. Transport of long and medium chain fatty acids by *Escherichia coli* K12. *J. Biol. Chem.* **256:** 3734–3742.
19. Black, P. N., S. F. Kianian, C. DiRusso, and W. D. Nunn. 1985. Long-chain fatty acid transport in *Escherichia coli.*: cloning, mapping, and expression of the *fadL* gene. *J. Biol. Chem.* **260:** 1780–1789.
20. Ginsburgh, C. L., P. N. Black, and W. D. Nunn. 1984. Transport of long chain fatty acids in *Escherichia coli*: identification of a membrane protein associated with *fadL* gene. *J. Biol. Chem.* **259:** 8437–8443.
21. Black, P. N. 1991. Primary sequence of the *Escherichia coli fadL* gene encoding an outer membrane protein required for long-chain fatty acid transport. *J. Bacteriol.* **173:** 435–442.
22. Kumar, G. B., and P. N. Black. 1991. Linker mutagenesis of a bacterial fatty acid transport protein: identification of domains with functional importance. *J. Biol. Chem.* **266:** 1–6.
23. Black, P. N., B. Said, C. R. Ghosn, J. V. Beach, and W. D. Nunn. 1987. Purification and characterization of an outer membrane-bound protein involved in long-chain fatty acid transport in *Escherichia coli*. *J. Biol. Chem.* **262:** 1412–1419.
24. Black, P. N. 1990. Characterization of *FadL*-specific fatty acid binding in *Escherichia coli*. *Biochim. Biophys. Acta.* **1046:** 97–105.
25. Kameda, K., L. K. Suzuki, and Y. Imai. 1985. Further purification, characterization and salt activation of acyl-CoA synthetase from *Escherichia coli*. *Biochim. Biophys. Acta.* **840:** 29–36.
26. Kameda, K. 1986. Partial purification and characterization of fatty acid binding protein(s) in *Escherichia coli* membranes and reconstitution of fatty acid transport system. *Biochem. Int.* **13:** 343–350.
27. Kameda, K., L. K. Suzuki, and Y. Imai. 1987. Transport of fatty acid is obligatory coupled with H^+ entry in spheroplasts of *Escherichia coli* K12. *Biochem. Int.* **14:** 227–234.
28. Azizan, A., and P. N. Black. 1994. Use of transposon Tn*phoA* to identify genes for cell envelope proteins of *Escherichia coli* required for long-chain fatty acid transport: the periplasmic protein Tsp potentiates long-chain fatty acid transport. *J. Bacteriol.* **176:** 6653–6662.
29. Schaffer, J. E., and H. F. Lodish. 1994. Expression cloning and characterization of a novel adipocyte long chain fatty acid transport protein. *Cell.* **79:** 427–436.
30. Stuhlsatz-Krouper, S. M., N. E. Bennett, and J. E. Schaffer. 1998. Substitution of alanine for serine 250 in the murine fatty acid transport protein inhibits long chain fatty acid transport. *J. Biol. Chem.* **273:** 28642–28650.
31. Schaffer, J. E., and H. F. Lodish. 1995. Molecular mechanism of long-chain fatty acid uptake. *Trends Cardiovasc. Med.* **5:** 218–224.
32. Man, M. Z., T. Y. Hui, J. E. Schaffer, H. F. Lodish, and D. A. Bernlohr. 1996. Regulation of the murine adipocyte fatty acid transport gene by insulin. *Mol. Endocrinol.* **10:** 1021–1028.
33. Martin, G., K. Schoonjans, A. Lefebvre, B. Staels, and J. Auwerx. 1997. Coordinate regulation of the expression of the fatty acid transport protein and acyl-CoA synthetase genes by PPAR. *J. Biol. Chem.* **272:** 28210–28217.
34. Frost, S. C., and D. M. Lane. 1985. Evidence for the involvement of vicinal sulfhydryl groups in insulin-activated hexose transport by 3T3-L1 adipocytes. *J. Biol. Chem.* **260:** 2646–2652.
35. Ory, D. S., B. A. Neugeborn, and R. C. Mulligan. 1996. A stable human-derived packaging cell line for production of high-titer retrovirus/vesicular stomatitis virus G psuedotype. *Proc. Natl. Acad. Sci. USA.* **93:** 11400–11406.
36. Simpson, I. A., D. R. Yver, P. J. Hissin, L. J. Wardzala, E. Karnieli, L. B. Salans, and S. W. Cushman. 1983. Insulin-stimulated translocation of glucose transporters in the isolated rat adipose cells: characterization of subcellular fractions. *Biochim. Biophys. Acta.* **763:** 393–407.
37. Tanaka, T., K. Hosaka, and S. Numa. 1981. Long-chain acyl-CoA synthetase from rat liver. *Methods Enzymol.* **71:** 334–341.
38. Moore, M. S., D. T. Mahaffey, F. M. Brodsky, and R. G. W. Anderson. 1987. Assembly of clathrin-coated pits onto purified plasma membranes. *Science.* **236:** 558–563.
39. Robinson, L. J., and D. E. James. 1992. Insulin-regulated sorting of glucose transporters in 3T3-L1 adipocytes. *Endocrinol. Metab.* **26:** E383–E393.
40. Heuser, J. E., and R. G. W. Anderson. 1989. Hypotonic media inhibit receptor-mediated endocytosis by blocking clathrin-coated pit formation. *J. Cell Biol.* **108:** 389–400.
41. Kansara, M. S., A. K. Mehra, J. von Hagen, E. Kabotyansky, and P. J. Smith. 1996. Physiological concentrations of insulin and T_3 stimulate 3T3-L1 adipocyte acyl-CoA synthetase gene transcription. *Am. J. Physiol.* **270:** E873–E881.
42. Elsing, C., W. Winn-Borner, and W. Stremmel. 1995. Confocal analysis of hepatocellular long-chain fatty acid uptake. *Am. J. Physiol.* **269:** G842–G851.
43. Kyte, J., and R. F. Doolittle. 1982. A simple method for displaying the hydropathic character of a protein. *J. Mol. Biol.* **157:** 105–132.
44. Robinson, L. J., S. Pang, D. S. Harris, J. Heuser, and D. E. James. 1992. Translocation of the glucose transporter (GLUT4) to the cell surface in permeabilized 3T3-L1 adipocytes: effects of ATP, insulin, and GTPγS and localization of GLUT4 to clathrin lattices. *J. Cell. Biol.* **117:** 1181–1196.
45. Lippel, K., J. Robinson, and E. G. Trams. 1970. Intracellular distribution of palmitoyl-CoA synthetase in rat liver. *Biochim. Biophys. Acta.* **206:** 173–177.
46. Farstad, M., J. Bremer, and K. R. Norum. 1967. Long-chain acyl Co-A synthetase in rat liver. A new assay procedure for the enzyme, and studies on its intracellular localization. *Biochim. Biophys. Acta.* **132:** 492–502.
47. Hesler, C. B., C. Olymbios, and D. Haldar. 1990. Transverse-plane topography of long-chain acyl-CoA synthetase in the mitochondrial outer membrane. *J. Biol. Chem.* **265:** 6600–6605.
48. Pande, S. V., and J. F. Mead. 1968. Long chain fatty acid activation in subcellular preparations from rat liver. *J. Biol. Chem.* **243:** 352–361.
49. Creasey, W. A. 1962. Observations on the activation of stearic acid by rat-liver preparations. *Biochim. Biophys. Acta.* **64:** 559–561.
50. Van Tol, A., and W. C. Hulsman. 1969. The localization of palmitoyl-CoA:carnitine palmitoyl transferase in rat liver. *Biochim. Biophys. Acta.* **189:** 342–353.
51. Shindo, Y., and T. Hashimo. 1978. Acyl-coenzyme A synthetase and fatty acid oxidation in rat liver peroxisomes. *J. Biochem.* **84:** 1177–1181.
52. Tanaka, T., K. Hosaka, M. Hoshimaru, and S. Numa. 1979. Purifi-

cation and properties of long-chain acyl-CoA synthetase from rat liver. *Eur. J. Biochem.* **98:** 165–172.
53. Krisans, S. K., and R. M. Mortenson. 1980. Acyl-CoA synthetase in rat liver peroxisomes. Computer-assisted analysis of cell fractionation experiments. *J. Biol. Chem.* **255:** 9599–9607.
54. de Jong, J. W., and H. W. Hulsman. 1970. A comparative study of palmitoyl-CoA synthetase activity in rat liver, heart, and gut mitochondrial and microsomal preparations. *Biochim. Biophys. Acta.* **197:** 127–135.
55. Ves-Losada, A., and R. R. Brenner. 1996. Long-chain fatty acyl-CoA synthetase enzymatic activity in rat liver cell nuclei. *Mol. Cell. Biochem.* **159:** 1–6.
56. Wanders, R. J. A., S. Denis, C. W. T. van Roermund, C. Jakobs, and H. J. ten Brink. 1992. Characteristics and subcellular localization of pristanoyl-CoA synthetase in rat liver. *Biochim. Biophys. Acta.* **1125:** 274–279.
57. Davidson, B. C., and R. C. Cantrill. 1985. Erythrocyte membrane acyl-CoA synthetase activity. *FEBS.* **193:** 69–74.
58. Davidson, B. C., and R. C. Cantrill. 1986. Rat hepatocyte plasma membrane acyl-CoA synthetase activity. *Lipids.* **21:** 571–574.
59. Morand, O., and M. Aigrot. 1985. Transport of fatty acids across the membrane of human erythrocyte ghosts. *Biochim. Biophys. Acta.* **835:** 68–76.
60. Lippel, K., and D. Blythe. 1972. Acyl-CoA synthetase activity associated with microsomal and mitochondrial contaminants of isolated rat liver nuclei. *Biochim. Biophys. Acta.* **280:** 231–234.
61. Mangroo, D., and G. E. Gerber. 1993. Fatty acid uptake in *Escherichia coli*: regulation by recruitment of fatty acyl-CoA synthetase to the plasma membrane. *Biochem. Cell Biol.* **71:** 51–56.
62. Luiken, J. J. F. P., F. A. van Nieuwenhoven, G. America, G. J. van der Vusse, and J. F. C. Glatz. 1997. Uptake and metabolism of palmitate by isolated cardiac myocytes from adult rats: involvement of sarcolemmal proteins. *J. Lipid Res.* **38:** 745–758.
63. Knudsen, J., P. Hojrup, H. O. Hansen, H. F. Hansen, and P. Roepstorff. 1989. Acyl-CoA-binding protein in the rat. Purification, binding characteristics, tissue concentrations and amino acid sequence. *Biochem. J.* **262:** 513–519.
64. Knoll, L. J., D. R. Johnson, and J. I. Gordon. 1995. Complementation of *Saccharomyces cerevisiae* strains containing fatty acid activation gene (*FAA*) deletions with a mammalian acyl-CoA synthetase. *J. Biol. Chem.* **270:** 10861–10867.
65. Johnson, D. R., L. J. Knoll, D. E. Levin, and J. I. Gordon. 1994. *Saccharomyces cerevisiae* contains four fatty acid activation (FAA) genes: an assessment of their role in regulating protein N-myristoylation and cellular lipid metabolism. *J. Cell Biol.* **127:** 751–762.
66. Johnson, D. R., L. J. Knoll, N. Rowley, and J. I. Gordon. 1994. Genetic analysis of the role of *Saccharomyces cerevisiae* acyl-CoA synthetase genes in regulating proteins N-myristoylation. *J. Biol. Chem.* **269:** 18037–18046.
67. Duronio, R. J., L. J. Knoll, and J. I. Gordon. 1992. Isolation of the *Saccharomyces cerevisiae* long chain fatty acyl:CoA synthetase gene (FAA1) and assessment of its role in protein N-myristoylation. *J. Cell Biol.* **117:** 515–529.
68. Miyazawa, S., T. Hashimoto, and S. Yokota. 1985. Identity of long-chain acyl-coenzyme A synthetase of microsomes, mitochondria, and peroxisomes in rat liver. *J. Biochem.* **98:** 723–733.
69. Fujino, T., K. Man-Jong, H. Minekura, H. Suzuki, and T. T. Yamamoto. 1997. Alternative translation initiation generates acyl-CoA synthetase 3 isoforms with heterogeneous amino termini. *J. Biochem.* **122:** 212–216.